ARTICLE

Controlling the Photoreactivity of the Photoactive Yellow Protein Chromophore by Substituting at the *p*-Coumaric Acid Group

Martial Boggio-Pasqua[†] and Gerrit Groenhof[*,‡]

[†]Laboratoire de Chimie et Physique Quantiques, IRSAMC, CNRS et Université de Toulouse, 31062 Toulouse, France
[‡]Computational Biomolecular Chemistry group, Max-Planck-Institut für Biophysikalische Chemie,
 Am Fassberg 11, D-37077 Göttingen, Germany

Ⓢ *Supporting Information*

ABSTRACT: We have performed ab initio CASSCF, CASPT2, and EOM-CCSD calculations on doubly deprotonated *p*-coumaric acid (pCA^{2-}), the chromophore precursor of the photoactive yellow protein. The results of the calculations demonstrate that pCA^{2-} can undergo only photoisomerization of the double bond. In contrast, the chromophore derivative with the acid replaced by a ketone (*p*-hydroxybenzylidene acetone, pCK^-) undergoes both single- and double-bond photoisomerization, with the single-bond relaxation channel more favorable than the double-bond channel. The substitution alters the nature of the

first excited states and the associated potential energy landscape. The calculations show that the electronic nature of the first two (π,π^*) excited states are interchanged in vacuo due to the substitution. In pCK^-, the first excited state is a charge-transfer (CT π,π^*) state, in which the negative charge has migrated from the phenolate ring onto the alkene tail of the chromophore, whereas the locally excited (LE π,π^*) state, in which the excitation involves the orbitals on the phenol ring, lies higher in energy and is the fourth excited state. In pCA^{2-}, the CT state is higher in energy due the presence of a negative charge on the tail of the chromophore, and the first excited state is the LE state. In isolated pCA^{2-}, there is a 68 kJ/mol barrier for double-bond photoisomerization on the potential energy surface of this LE state. In water, however, hydrogen bonding with water molecules reduces this barrier to 9 kJ/mol. The barrier separates the local trans minimum near the Franck—Condon region from the global minimum on the excited-state potential energy surface. The lowest energy conical intersection was located near this minimum. In contrast to pCK^-, single-bond isomerization is highly unfavorable both in the LE and CT states of pCA^{2-}. These results demonstrate that pCA^{2-} can only decay efficiently in water and exclusively by double-bond photoisomerization. These findings provide a rationale for the experimental observations that pCA^{2-} has both a longer excited-state lifetime and a higher isomerization quantum yield than pCK^-.
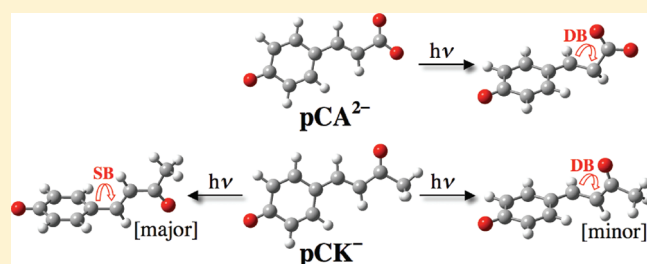
■ INTRODUCTION

The photoactive yellow protein (PYP) is assumed to be the primary photoreceptor for the photoavoidance response of the salt-tolerant bacterium *Halorhodospira halophila*.[1] PYP contains a deprotonated 4-hydroxy-cinnamic acid (or *p*-coumaric acid, pCA) chromophore linked covalently to the γ-sulfur of Cys69 via a thioester bond. Upon absorbing a blue-light photon, PYP enters a fully reversible photocycle involving several intermediates on time scales ranging from a few hundred femtoseconds to seconds.[2] In previous work, we have used mixed quantum/classical (QM/MM) simulations to reveal the detailed sequence of structural changes that follows photoabsorption in PYP.[3] The first step is a photoisomerization of the chromophore around its double bond, which has also been observed in several experimental studies.[4-7] In the protein, radiationless decay is very efficient because the intersection seam between the ground- (S_0) and excited-state (S_1) surfaces is located very near the minima on the excited-state potential energy surface. In the isolated chromophore, in contrast, the seam lies far from the minima. Hydrogen-bond interactions with the amino

acids in the chromophore pocket were found to cause the displacement of the seam.[8,9]

To understand how different environments influence the isomerization process, we have more recently performed calculations on a chromophore analogue (*p*-coumaric ketone (pCK^-), Figure 1) in water and in vacuo.[8] In both situations the predominant relaxation process in S_1 involves a rotation of the single bond (SB), adjacent to the ring (Figure 1), rather than rotation of the double bond (DB). In vacuo, only the double-bond rotation can lead to radiationless decay, whereas in water both channels lead to decay. Both the single- and double-bond twisted structures are minima on the excited-state potential energy surface but only in water is the S_1/S_0 seam lying near these minima.[8-10] The origin for the displacement of the seam is
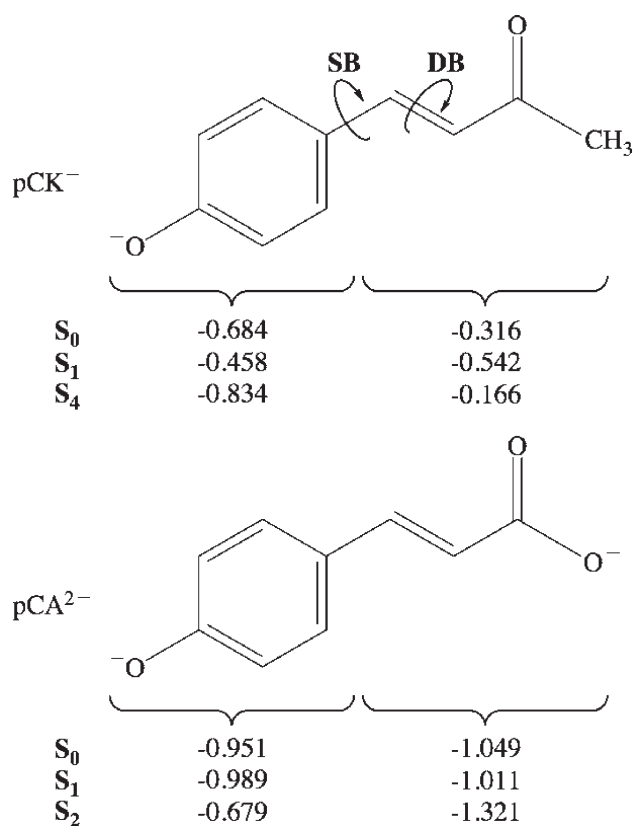
Figure 1. Representation of the two PYP chromophore analogues used in this study: the deprotonated *p*-coumaric ketone (pCK$^-$) and the doubly deprotonated *p*-coumaric acid (pCA^{2-}). Rotations around the single bond (SB) and double bond (DB) are shown. Mulliken charge distributions of the ground state and first two (π,π^*) excited states at the ground-state geometry are indicated.

an electrostatic stabilization of the chromophore's excited state by hydrogen-bond interactions with water molecules.[8,9]

Because single-bond photoisomerization is strongly favored over double-bond photoisomerization for pCK$^-$ in water, the probability of finding the chromophore in the cis configuration is very low.[8] This result is in good agreement with the very low isomerization quantum yield observed by Espagne and co-workers.[11] In their time-resolved fluorescence experiments, the excited-state lifetime was measured for a series of chromophore derivatives with different substituents at the *p*-coumaric acid group. The pCK$^-$ chromophore, with a methyl substituent (Figure 1), was found to decay the fastest (∼1 ps), albeit with a negligible trans-to-cis photoisomerization quantum yield. The doubly deprotonated *p*-coumaric acid chromophore (pCA^{2-}, Figure 1) had the longest S$_1$ lifetime (∼10 ps) and a much higher quantum yield.

To explain these differences from an electronic structure perspective, we have explored the excited-state decay channels in these chromophores by means of multiconfigurational ab initio computations. The results of our calculations demonstrate that in vacuo the electronic nature of the first two (π,π^*) excited states (S$_1$ and S$_2$) in pCA^{2-} is essentially opposite to that in pCK$^-$ (S$_1$ and S$_4$). Whereas pCK$^-$ predominantly relaxes into the single-bond twisted S$_1$ minimum, such a minimum does not exist in pCA^{2-}. Instead, there is only the double-bond twisted S$_1$ minimum in pCA^{2-}. In the isolated chromophore, this minimum is separated from the Franck–Condon region by a relatively high barrier. The

origin of this barrier is nonadiabatic coupling between the first (S$_1$) and the second excited state (S$_2$). By selectively stabilizing the S$_2$ charge-transfer (CT) state, hydrogen-bonding interactions with water molecules significantly lower this barrier, so that photoisomerization becomes efficient in water.

■ COMPUTATIONAL DETAILS

The lowest electronic singlet states of pCA^{2-} in vacuo and in water have been studied using a combination of ab initio methods. Triplet states have not been considered in this study, as they play a minor role.[12] A method describing the important electronic reorganization taking place in the different states is necessary to capture their electronic and structural features. The complete active space self-consistent field (CASSCF) method[13] is the most widely used multiconfigurational method in this respect. However, CASSCF calculations for pCA^{2-} would require a (14e,12o) active space including all the π and π^* orbitals. This size of active space is too large for a detailed study of the topology of the potential energy surfaces. A CASSCF calculation performed with such a large active space revealed that we could reduce the size to (12e,11o) without affecting significantly the results (Figure S1 of the Supporting Information). With this slightly smaller active space, geometry optimizations of critical points including conical intersections and harmonic vibrational frequency analyses are affordable. We employed a similar active space to perform the calculations on the pCK$^-$ chromophore (as used in ref 8).

To explore the topology of the potential energy surfaces along the excited-state relaxation pathways, we have performed linearly interpolated transit path calculations. Intermediate geometries were constructed by interpolating between the relevant optimized geometries in internal coordinates. To simulate the single-bond twist relaxation pathway, we interpolated between the S$_0$ minimum, the S$_1$ planar minimum, and the single-bond twisted S$_1$-optimized structures. For the double-bond twisted relaxation pathway, the linear interpolation was carried out between the S$_0$ minimum, the S$_1$ planar minimum, and the double-bond twisted S$_1$-optimized structures. To explore the possibility that the relaxation involves a concerted rotation of both double and single bonds, such a pathway was also investigated. We note that a linear transit path is a crude approximation of the true minimum energy reaction pathway and can only provide an upper-bound estimate of a barrier. However, a maximum identified on a linearly interpolated pathway usually provides a good starting geometry for a more rigorous transition state optimization. With the maximum energy structures found by the linear interpolations, we were thus able to optimize transition states and accurately determine the transition state barriers involved in the excited-state relaxation of the chromophores.

We also investigated the role of the lowest energy singlet (n,π^*) state by computing its energy profile for both single- and double-bond twist pathways at the equation-of-motion coupled cluster singles and doubles (EOM-CCSD) level of theory.[14] The minimum energy structure on the (n,π^*) state was further energy minimized at the CASSCF(14,12) level, with the relevant non-bonding orbital added into the active space. Subsequently, the energy at this geometry was reevaluated at the EOM-CCSD level again to confirm that the (n,π^*) state of pCA^{2-} has indeed a low-lying excited-state minimum, as in the neutral pCA chromophore.[15]

To correct for the lack of dynamic electron correlation at the CASSCF level, potential energies were recomputed along the main

7022

dx.doi.org/10.1021/jp108977x |*J. Phys. Chem. B* 2011, 115, 7021–7028

excited-state relaxation pathways of pCA^{2-} by employing both multi-configurational second-order perturbation theory (CASPT2)[16] and EOM-CCSD. The CASPT2 computations were performed using the (12e,11o) reference active space with orbitals averaged over all computed electronic states. A level-shift of 0.3 hartree was adopted to avoid intruder state problems in the excited-state calculations. Figures S2 and S3 of the Supporting Information show a qualitative good agreement of the CASSCF results (Figure S3) with both EOM-CCSD (Figure S2) and CASPT2 (Figure S3) results.

As we have shown previously for the pCK^- chromophore,[8] specific hydrogen-bond interactions can influence dramatically the excited-state relaxation pathways. To investigate if hydration has a similar effect on the excited state of pCA^{2-}, we explicitly included eight water molecules at key positions around the chromophore in our CASSCF computations. The starting geometry was taken from a ground-state QM/MM molecular dynamics simulation of the chromophore in a periodic box of water. In this simulation, the chromophore was described at the CASSCF(6,6)/3-21G level, and the water molecules were modeled by the SPCE potential.[17] The simulation was carried out with the Gromacs molecular dynamics program.[18] Because at least eight water molecules were found to donate a hydrogen bond to the chromophore in the trajectory, eight water molecules were selected from the last snapshot of the 5 ps simulation. The coordinates of the chromophore and the eight water molecules were fully optimized in our excited-state optimizations of minima, transition states, and conical intersections. Thus, we have neglected the effect of dynamic fluctuations of the water molecules on the photochemistry of pCA^{2-}. Although this is clearly an approximation, we believe it provides a clear physical insight into the effect of hydrogen-bond interactions.

Ideally, one would want to perform QM/MM excited-state dynamics simulations of pCA^{2-} in water, as was done previously for the pCK^- chromophore. However, because the time scale of the excited-state process is an order of magnitude longer and the minimal active space required to describe the excited-state potential energy surface is larger than in our previous application on pCK^-, such computations are beyond the reach of our computational resources.

To estimate the stability of the chromophore with respect to spontaneous electron emission, we calculated the energy difference before and after instantaneous removal of an electron from pCA^{2-} at various levels of theory.

The 6-31G(d)[19] basis set was used in all of the CASSCF calculations, whereas the CASPT2 and EOM-CCSD calculations were performed with the correlation-consistent cc-pVDZ[20] basis set. The effect of including diffuse functions was tested at the CASSCF and CASPT2 levels of calculation and did not show any change in the ordering of the lowest two (π,π^*) excited states (Table S1 of the Supporting Information). All of the ab initio calculations were performed with MOLPRO[21] and Gaussian.[22]

■ RESULTS AND DISCUSSION

Effect of Substitution on Electronic Structures. Before comparing the electronic structures of pCK^- and pCA^{2-} in vacuo, we want to make clear that the isolated pCA^{2-} chromophore only serves as a model system. As shown in Table S2 of the Supporting Information, the energy of the oxidized pCA^- radical lies below that of pCA^{2-} at all levels of theory employed. Therefore, the isolated pCA^{2-} is unstable with respect to spontaneous autoionization and cannot exist in the gas phase. In the hydrated environment, the
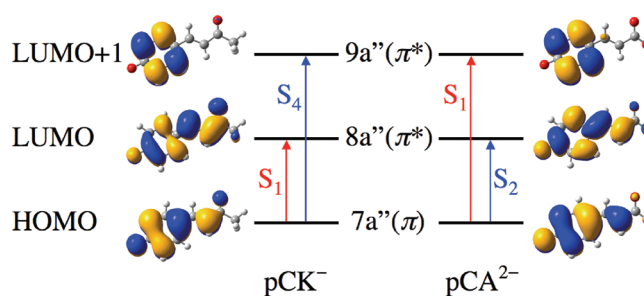

Figure 2. Relevant valence orbitals involved in the lowest $\pi \rightarrow \pi^*$ transitions in the pCK^- and pCA^{2-} chromophores. The orbitals are labeled according to the symmetry of the C_s point group.

dianion is stable toward autoionization and can thus exist. However, to understand the effect of the water molecules on the photochemistry of pCA^{2-} we need the hypothetical chromophore in vacuo as a reference.

All CASSCF-optimized structures and energies are collected in Figure S1 and Table S3 of the Supporting Information. EOM-CCSD relative energies computed at these CASSCF-optimized structures are collected in Table 1. The first two singlet (π,π^*) excited states of pCK^- (S_1 and S_4)[23] and pCA^{2-} (S_1 and S_2) at their optimized ground-state geometries have been computed. The molecular orbitals that contribute most to the two $\pi \rightarrow \pi^*$ excitation energies are shown in Figure 2. From a visual inspection, we conclude that the electronic nature of the first (π,π^*) excited state in pCA^{2-} is similar to the nature of the second (π,π^*) excited state in pCK^-, whereas the second excited state in pCA^{2-} corresponds to the first in pCK^-. In pCK^-, the $S_0 \rightarrow S_1$ transition involves an electron being promoted from the $7a''$ highest occupied molecular orbital into the $8a''$ lowest unoccupied molecular orbital. In pCA^{2-}, the $S_0 \rightarrow S_1$ transition is associated with an electron being promoted from the $7a''$ into the $9a''$ orbital. Thus, whereas in pCK^- S_1 corresponds to a HOMO → LUMO transition, in pCA^{2-} S_1 corresponds to a HOMO → LUMO + 1 transition. In this respect, the dianionic form of the p-coumaric acid group is remarkably similar to the neutral form, for which the S_1 state also corresponds to the HOMO → LUMO + 1 transition.[15,24]

Although in the ground state the energetic ordering of the virtual molecular orbitals is identical for the two chromophores, this order interchanges in pCA^{2-} when these orbitals become occupied with an electron. The $8a''$ orbital is delocalized over the whole chromophore, whereas the $9a''$ orbital is localized mainly on the phenolate ring. Promoting an electron into the $8a''$ orbital from $7a''$ thus corresponds to a partial charge-transfer (CT) excitation with some negative charge displaced from the ring onto the tail of the chromophore, as shown by the charge distributions in Figure 1. In pCK^-, which has a neutral tail group, this CT state is the lowest energy excited state (S_1). In contrast, because of the electrostatic repulsion between an electron in $8a''$ and the negatively charged carboxylate group, the $7a'' \rightarrow 8a''$ CT state in pCA^{2-} is higher in energy than the $7a'' \rightarrow 9a''$ transition that is more localized on the ring (LE state). Thus, the CT state in pCA^{2-} corresponds to the S_2 state, which is confirmed by the charge distributions shown in Figure 1. This situation is also similar to that in the neutral p-coumaric acid chromophore, in which the S_2 state also corresponds to the HOMO → LUMO CT state.[15,24] Moreover, the intensities of these transitions are comparable for both forms of the

Table 1. EOM-CCSD/cc-pVDZ Relative Energies at Selected Optimized Geometries of pCA^{2-} in Vacuo^a

	$\Delta E(S_0)$	$\Delta E(S_1)$	$\Delta E(S_2)$	$\Delta E(S_3)$
S_0 planar structure	0	395.1 (4.097) (π,π^*)	449.4 (4.660) (π,π^*)	478.7 (4.964) (n,π^*)
S_1 planar structure	17.5 (0.182)	371.6 (3.854) (π,π^*)	448.1 (4.647) (π,π^*)	490.4 (5.085) (n,π^*)
S_1 single-bond twisted structure	42.8 (0.444)	401.1 (4.159) (π,π^*)	499.2 (5.176) (n,π^*)	520.5 (5.397) (n,π^*)
S_1 double-bond twisted structure	332.4 (3.447)	338.6 (3.511) (π,π^*)	543.2 (5.633) (n,π^*)	580.6 (6.020) (n,π^*)
S_2 planar structure	11.3 (0.118)	386.2 (4.005) (π,π^*)	426.0 (4.417) (π,π^*)	446.5 (4.630) (n,π^*)
$S_1(n,\pi^*)$ planar structure	132.3 (1.372)	383.7 (3.979) (n,π^*)	494.1 (5.123) (π,π^*)	519.9 (5.391) (π,π^*)

^{a} The relative energies are given in kJ/mol and in eV (in parentheses). The structures used to compute these relative energies are the CASSCF-optimized structures found in Table S3 and Figure S1 of the Supporting Information. The EOM-CCSD potential energies can be found in Table S4 of the Supporting Information. The nature of the states is also indicated.
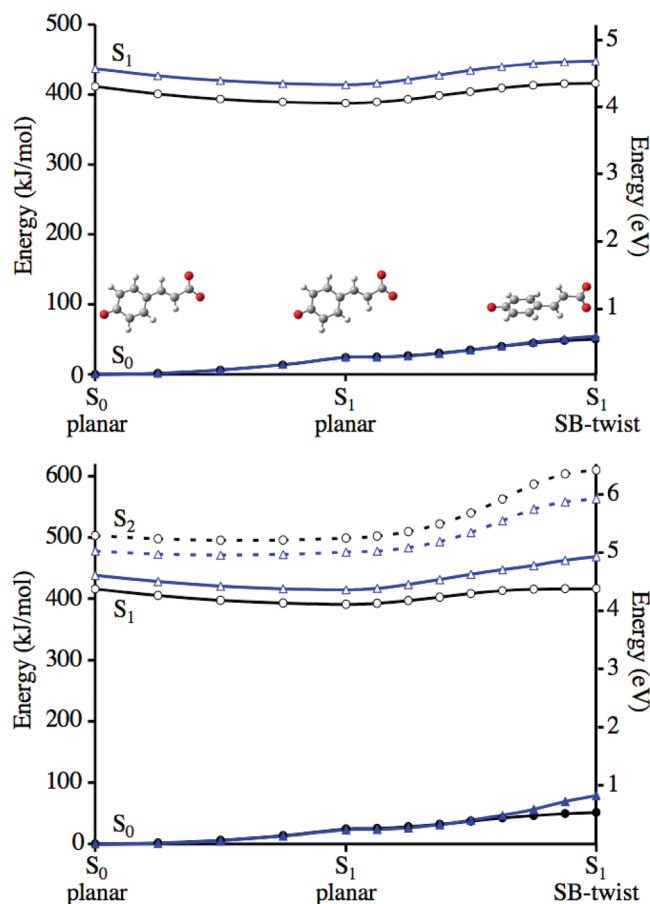

Figure 3. Two-state (top) and three-state (bottom) CASSCF potential energy profiles with (blue triangles) and without water (black circles) for the single-bond isomerization reaction in pCA^{2-}. The optimized structures used for the linearly interpolated transit path calculations in vacuo are shown.

chromophore. On the basis of the oscillator strengths evaluated at the EOM-CCSD level, the intensity of the $S_0 \rightarrow S_2$ transition is about 1 order of magnitude stronger than the $S_0 \rightarrow S_1$ transition in the neutral form.[15] We observed the same ratio for the dianionic form: the oscillator strengths, evaluated at the CASSCF level of theory, were found to be 0.095 and 0.717 for the $S_0 \rightarrow S_1$ and $S_0 \rightarrow S_2$ transitions, respectively. Thus, both of the S_1 and S_2 states can become populated upon photon absorption. Therefore, both states were considered for describing the photoisomerization process of the chromophore. For the neutral

chromophore, Martínez and co-workers demonstrated that within 50 fs after excitation to S_2, the chromophore decays to S_1.[24] Several low-lying S_2/S_1 conical intersections were identified in neutral pCA that involve only bond alteration.[24] In contrast, in fully deprotonated pCA^{2-} the lowest energy S_2/S_1 conical intersection was found near the double-bond twisted geometry (discussion below). There also exists an S_2/S_1 crossing with a planar conformation but it lies 52 kJ/mol above the S_2 planar minimum. Therefore, we do not expect that, after excitation to S_2, an ultrafast decay will take place to S_1 before the isomerization starts.

The third excited state (S_3) in pCA^{2-} is of (n,π^*) nature. Optimizing the geometry of this state leads to a planar minimum, for which the (n,π^*) state is lower in energy than the two (π,π^*) states discussed above (Table 1 and Table S4 of the Supporting Information). Thus, the $S_3(n,\pi^*)$ Franck−Condon state crosses the $S_1(\pi,\pi^*)$ and $S_2(\pi,\pi^*)$ states and leads to a second S_1 planar minimum. However, the lowest energy planar S_1 minimum corresponds to a (π,π^*) state (Table 1 and Table S4 of the Supporting Information), which lies 12 kJ/mol below the planar (n,π^*) S_1 minimum at the EOM-CCSD level. Again, the situation is similar to that in neutral pCA, which has also a low-lying (n,π^*) electronic state.[15]

Single-Bond Photoisomerization. In pCK$^-$, both single- and double-bond photoisomerizations are possible. The 90°-twisted single-bond and 90°-twisted double-bond geometries are both minima on the first excited-state potential energy surface.[8] The more favorable relaxation channel on the S_1 surface is a rotation of the formal single bond rather than of the double bond because the barrier to double-bond rotation is higher (Supporting Information in ref 8).

As shown in Figure 3, there exists no 90°-twisted single-bond S_1 minimum in pCA^{2-}. On the contrary, this structure is a transition state both in S_1 and in S_0 (Figure S4 of the Supporting Information). Because this transition state lies 28 kJ/mol above the planar local minimum in S_1, twisting the single bond is an activated process in pCA^{2-}, whereas it is barrierless in pCK$^-$.[8] Figure 4 illustrates the difference in the nature of the S_1 excited state at the single-bond twisted configurations. Whereas in pCK$^-$ the S_1 state is of clear CT nature, in pCA^{2-} the excitation involves only orbitals on the phenolate ring (LE state).

The absence of an accessible single-bond torsion S_1 relaxation channel in pCA^{2-} can be intuitively explained in terms of mesomerism using a simple valence bond picture as shown in Scheme 1. For the pCK$^-$ chromophore, two main valence bond structures can be drawn and the electronic structure can be seen as a mixture between the phenolate and quinone-like configurations.[9] In pCK$^-$, the negative charge is delocalized over the whole chromophore and the single bond adjacent to the ring has a partially
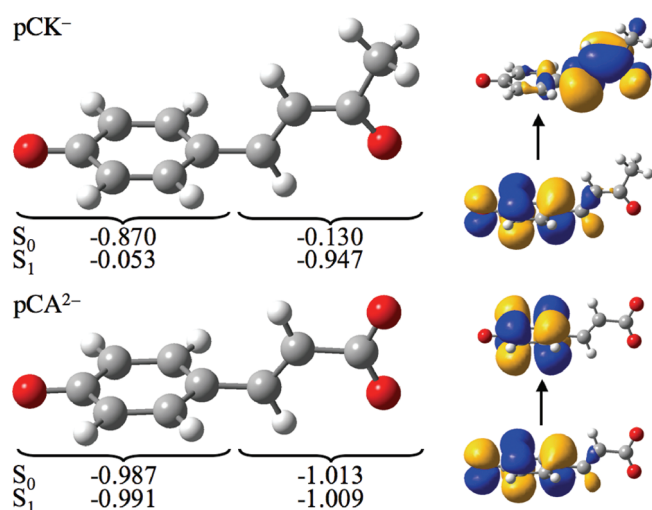
pCK⁻

S_0	-0.870	-0.130
S_1	-0.053	-0.947

pCA²⁻

S_0	-0.987	-1.013
S_1	-0.991	-1.009

Figure 4. Mulliken charge distributions of the S_0 and S_1 states at the single-bond twisted S_1 structure for pCK⁻ (top) and pCA²⁻ (bottom). The orbitals involved in the S_1 single excitation are shown, illustrating the charge-transfer and locally excited natures of the S_1 state in pCK⁻ and pCA²⁻, respectively.

Scheme 1. Main Valence Bond Structures for pCK⁻ (Top) and pCA²⁻ (Bottom) Chromophores[a]

[a] The minor quinone-like valence bond structure of pCA²⁻ is shown in gray.

double-bond character due to the significant quinone-like nature of the resonance structure (Scheme 1). This double-bond character is consistent with the optimized bond length of 1.43 Å, which is about the average of a single and double bond. In pCA²⁻, three main valence bond configurations can be drawn. The quinone-like valence bond structure has the two formal negative charges localized on the two oxygen atoms of the carboxylate group. Because of electrostatic repulsion, the latter configuration has a higher energy than the two other valence bond structures that have a maximal distance between the two formal charges (Scheme 1). Thus, the quinone-like structure should only make a very small contribution to the overall resonance structure. Therefore, the single bond adjacent to the ring in pCA²⁻ is not expected to have a substantial double-bond character, which is confirmed by the optimized bond length found at 1.48 Å in this chromophore (Figure S1 of the Supporting Information). If the favorable single-bond excited-state torsion pathway can be accounted for by the partial quinone-like character of the chromophore as found in pCK⁻,[9] then the lack of such character in pCA²⁻ can be used to explain the unfavorable nature of such pathway in this chromophore.

Because direct population of the $S_2(\pi,\pi^*)$ state cannot be ruled out (discussion above), we have also computed the potential energy profile of this state along the single-bond twisting pathway (Figure 3 for CASSCF profiles and Figure S2 of the Supporting Information for EOM-CCSD profiles). Like on S_1, there is also a large barrier to single-bond rotation on S_2. From the energy difference between the $S_2(\pi,\pi^*)$ energies at the planar and single-bond twisted structures optimized at the CASSCF level (Table S3 of the Supporting Information), we estimate that the barrier for single-bond twisting is 53 kJ/mol on S_2. Thus, initial photoexcitation to the S_2 state will also not lead to single-bond photoisomerization.

To find out whether radiationless $S_2(\pi,\pi^*) \rightarrow S_1(\pi,\pi^*)$ transitions are possible, we searched for conical intersections between these states at points along the single-bond isomerization path. Such intersections were indeed found near the planar and single-bond twisted S_2 geometries (Figure S1 of the Supporting Information) but were too high in energy to be accessible: 52 and 54 kJ/mol above the S_2 planar minimum, respectively (Table S3 of the Supporting
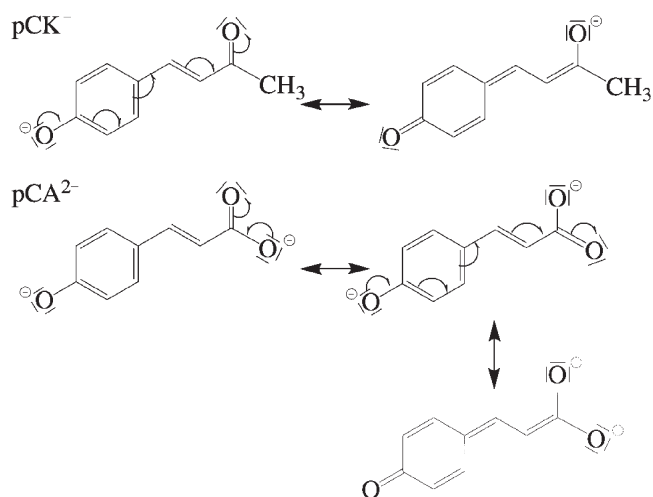
Information). Alternatively, the $S_2(\pi,\pi^*)$ may decay via the (n,π^*) state. As shown in the EOM-CCSD potential energy profiles (Figure S2 of the Supporting Information), the $S_2 (\pi,\pi^*)$ state intersects the (n,π^*) state along the single-bond isomerization pathway. Optimization of the conical intersection between these states demonstrates that the crossing has still a planar structure and lies less than 1 kJ/mol above the planar S_2 minimum at the CASSCF level (Table S3 of the Supporting Information). Therefore, after excitation to S_2, decay could readily occur to the (n,π^*) state via this low-lying conical intersection. Furthermore, we have also located a conical intersection with a planar geometry between the (n,π^*) state and the $S_1(\pi,\pi^*)$ state that lies 21 kJ/mol above the planar S_1 minimum at the CASSCF level (Table S3 of the Supporting Information).

Again, this situation is very similar to that in the neutral pCA chromophore.[15,24] As it was proposed for the neutral chromophore,[24] the (n,π^*) state may become populated if the excitation energy is increased. The rationale for such mechanism is that after direct excitation to S_2, fast nonradiative decay takes place to the (n,π^*) state via the aforementioned low-lying conical intersection. However, as in neutral pCA, the (n,π^*) state is unlikely to be involved in the isomerization process.[24]

Double-Bond Photoisomerization. Having excluded the single-bond isomerization channel in pCA²⁻, we now turn our attention to the photoisomerization of the double bond. In isolated pCA²⁻, isomerization in the first excited state is a highly activated process (Figure 3). The height of the barrier is 102 kJ/mol on the interpolated pathway. However, this is an upper-bound value due to the approximate nature of this pathway. Subsequent optimization of the geometry corresponding to this barrier yields a transition state that is 68 kJ/mol higher in energy than the local trans minimum (transition state structure in Figure S1 of the Supporting Information). Interestingly, this barrier is significantly larger than the barrier found for the neutral pCA chromophore: 18.6 kJ/mol at CASSCF level and 8.9 kJ/mol at CASPT2 level using a reduced (6e,5o) active space, state-averaged orbitals over 5 states, and a fixed torsion angle.[24]

The origin for the S_1 barrier is a strong nonadiabatic coupling between the S_1 and S_2 states (Figure 5). This coupling induces
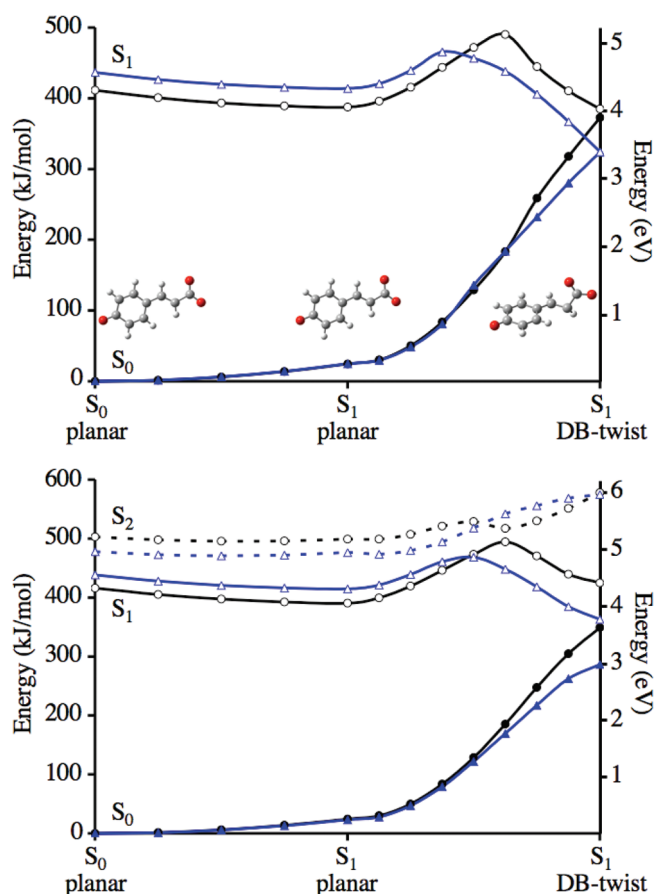
Figure 5. Two-state (top) and three-state (bottom) CASSCF potential energy profiles with (blue triangles) and without water (black circles) for the double-bond isomerization reaction in pCA^{2-}. The avoided crossing between the S_1 and S_2 states is clearly visible, as well as the narrowing of the gap between these two states in water. Note that, because state-averaging over three states was used in the bottom figure, the S_1/S_0 degeneracy is lifted at the double-bond twisted conical intersection in water.

an avoided crossing between the adiabatic surfaces that correspond to the $7a'' \rightarrow 9a''$ (S_1) and the $7a'' \rightarrow 8a''$ (S_2) excited states (Figure 2). Such coupling was also reported previously for the neutral pCA chromophore.[15,24] In neutral pCA, a conical intersection exists near this barrier and it was proposed that the experimental observation[25] of the decrease in isomerization efficiency upon increasing the excitation energy is due to a diabatic trapping at this S_2/S_1 intersection.[24] Note, however, that this experimental observation was later attributed to the isomerization in p-vinylphenol rather than in trans-pCA.[26]

A second consequence of the coupling between S_1 and S_2 is that after passing the barrier, the nature of the S_1 state corresponds to the $7a'' \rightarrow 8a''$ states, as in pCK$^-$ (Figure S5 of the Supporting Information). Near the double-bond twisted S_1 minimum, this state crosses with the S_0 state (Figure 3). The minimum energy S_1/S_0 conical intersection point has a sloped topology,[27] that is, the gradients of both surfaces are almost parallel at the crossing (Figure S6 of the Supporting Information).

Although the S_1/S_0 conical intersection near the double-bond twisted minimum lies far below the Franck−Condon energy, it is not easily accessed due to the large barrier that separates this intersection point from the Franck−Condon

region. Alternatively, because of the relatively low barrier for a 180° rotation of the single bond we also searched for conical intersection involving a combined rotation of both torsion angles. Such hula-twist conical intersection exists (Figure S1 of the Supporting Information) but lies 109 kJ/mol higher in energy than the double-bond twisted conical intersection in vacuo (174 kJ/mol in water). Because the energy required to access this crossing is much higher than the transition state for double-bond twisting, we consider the decay via a hula-twist pathway very unlikely.

Finally, we also searched for a prefulvene-like S_1/S_0 conical intersection involving a kinked benzene ring, which in neutral pCA provides an energetically accessible decay channel.[24] Such prefulvene-like conical intersection also exists in pCA^{2-} but is 142 kJ/mol higher in energy than the planar S_1 minimum (Table S3 and Figure S1 of the Supporting Information). Therefore, we do not expect this crossing to play a role in the photochemistry of the doubly deprotonated chromophore.

As discussed before, direct population to S_2 is also possible. Isomerization around the double bond on S_2 involves a barrier that is smaller than the barrier on S_1 (Figure 5). Furthermore, we could locate a conical intersection between the S_2 and S_1 surfaces along the isomerization pathway that is only 10 kJ/mol higher in energy than the planar S_2 minimum (Table S3 of the Supporting Information). Therefore, if S_2 is excited with sufficient energy, the initial phase isomerization could take place on S_2, rather than S_1. During the isomerization toward the double-bond twisted structure, a radiationless decay via the S_2/S_1 conical intersection, followed by a second decay at the S_1/S_0 intersection near the S_1 double-bond twisted minimum, provides an alternative scenario for the radiationless deactivation from the S_2 state. However, radiationless decay from S_2 to the (n,π^*) state at the planar conical intersection (discussion above and Table S3 of the Supporting Information) provides a competitive pathway that could inhibit double-bond isomerization on S_2. In addition to possible diabatic trapping in the S_2 state observed by Martínez and co-workers in neutral pCA,[24] the trapping of the system in the (n,π^*) state could potentially also contribute to a lowering of the isomerization efficiency upon increasing the excitation energy.

Effect of Hydration. In pCK$^-$, hydrogen-bond interactions between the chromophore and water molecules selectively stabilize the S_1 excited state.[8] Because the nature of the S_2 state in pCA^{2-} corresponds to the S_1 (CT) state in pCK$^-$, we expect a similar effect on the S_2 state in pCA^{2-}. Furthermore, the solvation may help stabilizing pCA^{2-} with respect to autoionization. To explore the effect of hydrogen bonding, we have repeated the geometry optimizations of the chromophore with eight water molecules included. The starting configuration of the chromophore and the water molecules was taken from a QM/MM molecular dynamics trajectory and only the water molecules that form hydrogen bonds with the chromophore were selected. As shown in Figure 5, the interactions with the water molecules indeed stabilize the S_2 state. In addition, the solvent effect also lowers the energy of pCA^{2-} with respect to the pCA$^-$ radical (Table S2 of the Supporting Information) by about 5 eV. Therefore, the S_1 and S_2 (π,π^*) states become stable with respect to autoionization, as the ionization energy is about 1 eV higher than the excitation energies to these states (Tables S1 and S5 of the Supporting Information).

Selective stabilization of the S_2 charge distribution by hydrogen bonding has no effect on the single bond rotation in pCA^{2-} (Figure 3). Neither in vacuo, nor in solution, a single-

bond twisted minimum exists on the S_2 potential energy surface. The hydrogen-bond interactions are not strong enough to stabilize two units of negative charge on the carboxylate moiety, in such a twisted intramolecular CT state. Furthermore, because there is not much difference in the overall charge distribution of the S_0 and S_1 states (Figure 4), the inclusion of water does not decrease the energy gap between the states, as it does in pCK$^-$.[8] Therefore, the interaction with the waters does not result in surface crossings between the S_1 and S_0 states along the single-bond isomerization pathway. Thus, whereas single-bond torsion provides a very efficient radiationless deactivation channel in hydrated pCK$^-$, this is not the case in pCA^{2-}.

The water has a much larger effect on the double-bond photo-isomerization of pCA^{2-}. Because of the avoided crossing between the adiabatic S_2 and S_1 potential energy surfaces, the selective stabilization of S_2 causes a significant stabilization of the transition state for double-bond photoisomerization, reducing the barrier from 68 to 9 kJ/mol (Table S3 of the Supporting Information). Because the energy of the Franck—Condon region is much higher than this barrier, the double-bond isomerization pathway is accessible in water. However, because the barrier to single-bond isomerization in pCK$^-$ is almost barrierless, the excited-state decay in water is slower for pCA^{2-} than for pCK$^-$, in agreement with time-resolved measurement on these chromophores.[11]

Because the electronic states have interchanged at the avoided crossing, the nature of the S_1 state in pCA^{2-} after crossing the barrier corresponds to that of the S_1 state in pCK$^-$ (Figure S5 of the Supporting Information). The hydrogen-bond interactions with the water molecules therefore also contribute to stabilizing the region around the double-bond twisted minimum on the S_1 surface with respect to the S_0 surface. In addition, the hydrogen bonds change the topology of the conical intersection from sloped in isolation to peaked in water (Figure S6 of the Supporting Information). Thus, after crossing the transition state, radiationless decay to the ground state is very efficient. Furthermore, with no competing single-bond isomerization channel available, the quantum yield for double-bond isomerization will be much higher than in pCK$^-$, as was measured experimentally by Espagne and co-workers.[11]

We have shown that hydrogen-bond interactions with water molecules can preferentially stabilize the CT state over the LE state. Despite this stabilization, the CT state remains higher in energy than the LE state at the CASSCF level, on which the results presented above are based. However, the EOM-CCSD and CASPT2 results show that also dynamic correlation stabilizes the CT state with respect to the LE state (Table S1 of the Supporting Information). Because our resources do not allow us to include dynamic correlation on the excitation energies of microsolvated pCA^{2-}, we cannot rule out that in reality the CT state lies below the LE state in solution.

To address this issue at least qualitatively, we performed time-dependent density functional theory (TD-DFT) calculations to estimate the order of excitation energies in isolated pCA^{2-} and in the microsolvated species, with a polarizable continuum model. Long-range-corrected hybrid functionals[28−30] and a double-hybrid density functional[31] were employed, but the observed trend was not sensitive to the functional (Table S5 of the Supporting Information). The TD-DFT results show that in the hydrated chromophore the CT state is lower than the LE state. The obtained transition energies are in fairly good agreement with the absorption maximum observed around 3.7 eV and

the shoulder around 4.0 eV.[11] Note that this shoulder was previously assigned to an (n,π^*) state in wild-type PYP.[32]

Note that even if the CT state is the lowest excited state in water, as the TD-DFT results suggest, the photoisomerization mechanism remains qualitatively the same. The CASSCF results predict that double-bond photoisomerization takes place on the LE state until the S_1 barrier is reached (Figure 5). After the barrier, the isomerization process continues on the CT state (Figure S5 of the Supporting Information). Thus, if the CT state were the lowest excited state throughout the isomerization process, only the initial stage of the excited-state relaxation process would be affected. However, because the potential energy profiles of the two states are rather similar, we would not expect a different mechanism. In both LE and CT states, rather high-energy barriers prevent single-bond photoisomerization. Furthermore, no stable single-bond twisted configuration exists in these states. Only the activated double-bond isomerization channel is accessible, which accounts for both a higher trans-to-cis isomerization quantum yield, as well as a longer excited-state lifetime of pCA^{2-} compared to pCK$^-$.

■ CONCLUSIONS

The results of the calculations presented here offer an explanation for the differences in the photochemistry of the pCK$^-$ and pCA^{2-} chromophores. Both the longer excited-state lifetime and higher quantum yield for double-bond isomerization in pCA^{2-} are a consequence of the unfavorable single-bond isomerization pathway in this dianionic chromophore. The S_1 potential energy surfaces are qualitatively different in pCA^{2-} and pCK$^-$. The calculations confirm the intuitive explanation proposed by Espagne and co-workers[11] in terms of the electron withdrawing strength of the substituent at the p-coumaric acid group of the chromophore. Because of its negative charge, the carboxylate group in pCA^{2-} is a very weak electron acceptor, whereas the neutral methyl-ketone group in pCK$^-$ is a much stronger acceptor. Because of this difference, the CT excited state is the lowest excited state in isolated pCK$^-$ but not in isolated pCA^{2-}. In pCK$^-$, relaxation on this CT state is possible via both single- and double-bond isomerization. In pCA^{2-}, the only relaxation channel is an activated double-bond photoisomerization in both the LE and CT states. In the hypothetical isolated pCA^{2-} chromophore, there is a high-energy transition state to double-bond photoisomerization. This transition state is a consequence of an avoided crossing between the S_1 LE and S_2 CT states. Selective stabilization of the CT state by hydrogen bonds lowers this barrier so that in water double-bond photoisomerization is an efficient decay process with a significant quantum yield. Thus, the coupling between the LE and CT states appears as one of the main driving forces for the excited-state population decay channel in this chromophore, as already stressed in previous studies.[11,33−35] Direct population of S_2 may not increase the isomerization quantum yield, as it opens up the channel to the (n,π^*) state.

■ ASSOCIATED CONTENT

ⓢ Supporting Information. Tables of transition energies including diffuse basis functions, first ionization energies, list of optimized Cartesian coordinates and energies with CASSCF, EOM-CCSD energies, and TD-DFT transition energies. Figures of CASSCF-optimized structures, EOM-CCSD potential energy profile, CASPT2 potential energy profile, transition state nature

7027

dx.doi.org/10.1021/jp108977x |J. Phys. Chem. B 2011, 115, 7021–7028

of the S_1 single-bond twisted structure, orbitals involved at the S_1 double-bond twisted structure, and the nature of the double-bond twisted S_1/S_0 conical intersection. This material is available free of charge via the Internet at http://pubs.acs.org.

■ AUTHOR INFORMATION

Corresponding Author
*E-mail: ggroenh@gwdg.de.

■ ACKNOWLEDGMENT

■ REFERENCES

(1) Hoff, W. D.; Dux, P.; Hard, K.; Devreese, B.; Nugteren-Roodzant, I. M.; Crielaard, W.; Boelens, R.; Kaptein, R.; van Beeumen, J.; Hellingwerf, K. J. *Biochemistry* **1994**, *33*, 13959–13962.

(2) Hellingwerf, K. J.; Hendriks, J.; Gensch, T. *J. Phys. Chem. A* **2003**, *107*, 1082–1094.

(3) Groenhof, G.; Bouxin-Cademartory, M.; Hess, B.; de Visser, S. P.; Berendsen, H. J. C.; Olivucci, M.; Mark, A. E.; Robb, M. A. *J. Am. Chem. Soc.* **2004**, *126*, 4228–4233.

(4) Heyne, K.; Mohammed, O. F.; Usman, A.; Dreyer, J.; Nibbering, E. T. J.; Cusanovich, M. A. *J. Am. Chem. Soc.* **2005**, *127*, 18100–18106.

(5) Kort, R.; Hellingwerf, K. J.; Ravelli, R. B. G. *J. Biol. Chem.* **2004**, *279*, 26417–26424.

(6) Ihee, H.; Rajagopal, S.; Srajer, V.; Pahl, R.; Anderson, S.; Schmidt, M.; Schotte, F.; Anfinrud, P. A.; Wulff, M.; Moffat, K. *Proc. Natl. Acad. Sci. U.S.A.* **2005**, *102*, 7145–7150.

(7) van Wilderen, L. J. G. W.; van der Horst, M. A.; van Stokkum, I. H. M.; Hellingwerf, K. J.; van Grondelle, R.; Groot, M. L. *Proc. Natl. Acad. Sci. U.S.A.* **2006**, *103*, 15050–15055.

(8) Boggio-Pasqua, M.; Robb, M. A.; Groenhof, G. *J. Am. Chem. Soc.* **2009**, *131*, 13580–13581.

(9) Gromov, E. V.; Burghardt, I.; Hynes, J. T.; Köppel, H.; Cederbaum, L. S. *J. Photochem. Photobiol., A* **2007**, *190*, 241–257.

(10) Virshup, A. M.; Punwong, C.; Pogorelov, T. V.; Lindquist, B. A.; Ko, C.; Martínez, T. J. *J. Phys. Chem. B* **2009**, *113*, 3280–3291.

(11) Espagne, A.; Paik, D. H.; Changenet-Barret, P.; Plaza, P.; Martin, M. M.; Zewail, A. H. *Photochem. Photobiol. Sci.* **2007**, *6*, 780–787.

(12) Coto, P. B.; Roca-Sanjuán, D.; Serrano-Andrés, L.; Martín-Pendás, A.; Martí, S.; Andrés, J. *J. Chem. Theory Comput.* **2009**, *5*, 3032–3038.

(13) Roos, B. O. *Adv. Chem. Phys.* **1987**, *69*, 399–445.

(14) Stanton, J. F.; Bartlett, R. J. *J. Chem. Phys.* **1993**, *98*, 7029–7039.

(15) Gromov, E. V.; Burghardt, I.; Köppel, H.; Cederbaum, L. S. *J. Phys. Chem. A* **2005**, *109*, 4623–4631.

(16) Celani, P.; Werner, H.-J. *J. Chem. Phys.* **2000**, *112*, 5546–5557.

(17) Berendsen, H. J. C.; Grigera, J. R.; Straatsma, T. P. *J. Phys. Chem.* **1987**, *91*, 6269–6271.

(18) van der Spoel, D.; Lindahl, E.; Hess, B.; Groenhof, G.; Mark, A. E.; Berendsen, H. J. C. *J. Comput. Chem.* **2005**, *26*, 1701–1718.

(19) (a) Hehre, W. J.; Ditchfield, R.; Pople, J. A. *J. Chem. Phys.* **1972**, *56*, 2257–2261. (b) Harihan, P. C.; Pople, J. A. *Theor. Chim. Acta* **1973**, *28*, 213–222.

(20) Dunning, T. H. *J. Chem. Phys.* **1989**, *90*, 1007–1023.

(21) Werner, H.-J.; Knowles, P. J.; Lindh, R.; Manby, F. R.; Schütz, M.; Celani, P.; Korona, T.; Mitrushenkov, A.; Rauhut, G.; Adler, T. B.; Amos, R. D.; Bernhardsson, A.; Berning, A.; Cooper, D. L.; Deegan, M. J. O.; Dobbyn, A. J.; Eckert, F.; Goll, E.; Hampel, C.; Hetzer, G.; Hrenar, T.; Knizia, G.; Köppl, C.; Liu, Y.; Lloyd, A. W.; Mata, R. A.; May, A. J.; McNicholas, S. J.; Meyer, W.; Mura, M. E.; Nicklass, A.; Palmieri, P.; Pflüger, K.; Pitzer, R.; Reiher, M.; Schumann, U.; Stoll, H.; Stone,

A. J.; Tarroni, R.; Thorsteinsson, T.; Wang, M.; Wolf, A. *MOLPRO*, version 2009.1, a package of ab initio programs, see http://www.molpro.net.

(22) Frisch, M. J.; Trucks, G. W.; Schlegel, H. B.; Scuseria, G. E.; Robb, M. A.; Cheeseman, J. R.; Scalmani, G.; Barone, V.; Mennucci, B.; Petersson, G. A.; Nakatsuji, H.; Caricato, M.; Li, X.; Hratchian, H. P.; Izmaylov, A. F.; Bloino, J.; Zheng, G.; Sonnenberg, J. L.; Hada, M.; Ehara, M.; Toyota, K.; Fukuda, R.; Hasegawa, J.; Ishida, M.; Nakajima, T.; Honda, Y.; Kitao, O.; Nakai, H.; Vreven, T.; Montgomery, Jr., J. A.; Peralta, J. E.; Ogliaro, F.; Bearpark, M. J.; Heyd, J. J.; Brothers, E.; Kudin, K. N.; Staroverov, V. N.; Kobayashi, R.; Normand, J.; Raghavachari, K.; Rendell, A.; Burant, J. C.; Iyengar, S. S.; Tomasi, J.; Cossi, M.; Rega, N.; Millam, N. J.; Klene, M.; Knox, J. E.; Cross, J. B.; Bakken, V.; Adamo, C.; Jaramillo, J.; Gomperts, R.; Stratmann, R. E.; Yazyev, O.; Austin, A. J.; Cammi, R.; Pomelli, C.; Ochterski, J. W.; Martin, R. L.; Morokuma, K.; Zakrzewski, V. G.; Voth, G. A.; Salvador, P.; Dannenberg, J.J.; Dapprich, S.; Daniels, A. D.; Farkas, Ö.; Foresman, J. B.; Ortiz, J. V.; Cioslowski, J.; Fox, D. J. *Gaussian 09*, Revision A.2; Gaussian, Inc., Wallingford CT, 2009.

(23) EOM-CCSD/cc-pVDZ transition energies are as follows: $S_0 \rightarrow S_1(CT\ \pi,\pi^*) = 3.302$ eV, $S_0 \rightarrow S_2(n,\pi^*) = 4.203$ eV, $S_0 \rightarrow S_3(n,\pi^*) = 4.340$ eV, $S_0 \rightarrow S_4(LE\ \pi,\pi^*) = 4.458$ eV.

(24) Ko, C.; Levine, B.; Toniolo, A.; Manohar, L.; Olsen, S.; Werner, H.-J.; Martínez, T. J. *J. Am. Chem. Soc.* **2003**, *125*, 12710–12711.

(25) Ryan, W. L.; Gordon, D. J.; Levy, D. H. *J. Am. Chem. Soc.* **2002**, *124*, 6194–6201.

(26) de Groot, M.; Buma, W. J. *J. Phys. Chem. A* **2005**, *109*, 6135–6136.

(27) Atchity, G. J.; Xantheas, S. S.; Ruedenberg, K. *J. Chem. Phys.* **1991**, *95*, 1862–1876.

(28) Yanai, T.; Tew, D. P.; Handy, N. C. *Chem. Phys. Lett.* **2004**, *393*, 51–57.

(29) Vydrov, O. A.; Scuseria, G. E. *J. Chem. Phys.* **2006**, *125*, 234109.

(30) Chai, J.-D.; Head-Gordon, M. *J. Chem. Phys.* **2008**, *128*, 084106. *Phys. Chem. Chem. Phys.* **2008**, *10*, 6615–6620.

(31) Grimme *J. Chem. Phys.* **2006**, *124*, 034108. S. Goerigk, L.; Moellmann, J.; Grimme, S. *Phys. Chem. Chem. Phys.* **2009**, *11*, 4611–4620.

(32) Borucki, B.; Otto, H.; Meyer, T. E.; Cusanovich, M. A.; Heyn, M. P. *J. Phys. Chem. B* **2005**, *109*, 629–633.

(33) Espagne, A.; Changenet-Barret, P.; Plaza, P.; Martin, M. M. *J. Phys. Chem. A* **2006**, *110*, 3393–3404.

(34) Espagne, A.; Paik, D. H.; Changenet-Barret, P.; Martin, M. M.; Zewail, A. H. *ChemPhysChem* **2006**, *7*, 1717–1726.

(35) Espagne, A.; Changenet-Barret, P.; Plaza, P.; Baudin, J.-B.; Martin, M. M. *J. Photochem. Photobiol., A* **2007**, *185*, 245–252.

7028

dx.doi.org/10.1021/jp108977x |*J. Phys. Chem. B* 2011, 115, 7021–7028